Hindawi Publishing Corporation
Case Reports in Medicine
Volume 2014, Article ID 786578, 6 pages
http://dx.doi.org/10.1155/2014/786578

Case Report

Pars Plana Vitrectomy Combined with Focal Endolaser Photocoagulation for Idiopathic Macular Telangiectasia

Gaku Terauchi,[1] Celso Soiti Matsumoto,[1,2] Kei Shinoda,[1] Harue Matsumoto,[2] Yutaka Imamura,[3] Emiko Watanabe,[1] Takaaki Kondo,[1] and Atsushi Mizota[1]

[1] *Department of Ophthalmology, Teikyo University School of Medicine, 2-11-1 Kaga, Itabashi-ku, Tokyo 173-0003, Japan*
[2] *Matsumoto Eye Clinic, Tokushima, Japan*
[3] *Department of Ophthalmology, Teikyo University School of Medicine, University Hospital Mizonokuchi, Kanagawa, Japan*

Correspondence should be addressed to Kei Shinoda; shinodak@med.teikyo-u.ac.jp

Received 14 August 2013; Revised 13 December 2013; Accepted 27 December 2013

Academic Editor: Marco A. Zarbin

Background. To report the outcome of pars plana vitrectomy (PPV) combined with intraoperative endolaser focal photocoagulation (PC) on eyes with idiopathic macular telangiectasis (MacTel) type 1. *Methods.* This was a retrospective study of two female patients with MacTel type 1 who were resistant to focal photocoagulation, sub-Tenon triamcinolone injection, and/or antiangiogenic drugs. The best-corrected visual acuity (BCVA) was determined, and fluorescein angiography (FA) and spectral domain optical coherence tomography (SD-OCT) were performed before and after surgery for up to 19 months. *Results.* After surgery, the BCVA gradually improved from 20/100 to 20/20 at 19 months in Case 1 and from 20/50 to 20/13 at 13 months in Case 2. Fluorescein angiography (FA) showed leakage at the late phase, and OCT showed that the cystoid macular edema was resolved and the fovea was considerably thinner postoperatively. *Conclusion.* Patients with MacTel type 1 who are refractory to the other types of treatments can benefit from PPV combined with intraoperative endolaser focal PC with functional and morphological improvements.

1. Introduction

Idiopathic juxtafoveal macular telangiectasia (MacTel) is characterized by vascular anomalies affecting the macular capillary network. It was first described by Gass and Oyakawa [1] and Gass and Blodi [2] and named idiopathic juxtafoveolar retinal telangiectasis (IJRT). It was recently renamed macular telangiectasis (MacTel) by Yannuzzi et al. [3]. There are two types of MacTel: type 1 with aneurysmal telangiectasia and type 2 with parafoveal telangiectasia. MacTel type 1 or unilateral parafoveal telangiectasis (Group 1B IJRT) typically occurs in one eye of relative young men. The temporal half of the macula is involved by the telangiectasis, and the macular oedema and hard exudates lead to vision reduction. No treatment has been established although some encouraging effects have been obtained by argon laser photocoagulation (PC) [4, 5], intravitreal or sub-Tenon's capsule injection of triamcinolone acetonide (IVTA or STTA) [5–7], or intravitreal bevacizumab (IVR) or ranibizumab (IVB) injections [8–10] in small case series.

We present two patients with MacTel type 1 who were refractory to photocoagulation (PC), STTA, and IVB but responded to pars plana vitrectomy (PPV) combined with intraoperative endolaser focal PC.

2. Materials and Methods

This was a retrospective study of two eyes of two patients with MacTel type 1 who did not respond to focal PC delivered by an integrated slit lamp, to STTA, and/or to IVB. After discussing the possible treatment options including repetition of earlier treatments, an informed consent was obtained for our technique of PPV combined with intraoperative endolaser focal PC. Both patients underwent PPV combined with endolaser focal PC during the surgery. The diagnosis of MacTel type 1 was based on the fundus examination, FA, and OCT after the exclusion of neovascular maculopathy,

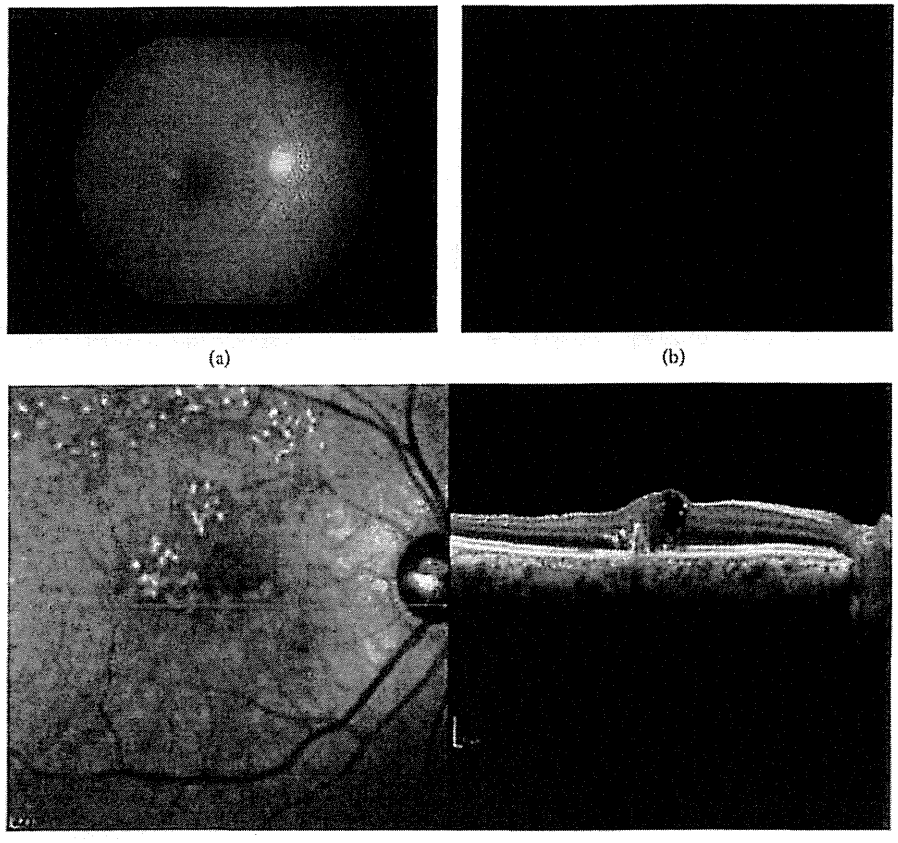

FIGURE 1: Finding of the right eye of Patient 1 with idiopathic macular telangiectasis (MacTel) type 1 on her first visit. Her best-corrected visual acuity (BCVA) was 20/100. (a) Fundus photograph showing hard exudates associated with telangiectasia temporal to the fovea. (b) Fluorescein angiogram showing strong fluorescein leakage in the late phase. (c) Optical coherence tomographic (OCT) image showing cystoid macular edema in the area surrounding the leakage.

secondary macular telangiectasia, and diabetes. Both eyes had cystoid macular oedema (CME) and showed a prompt filling of both the superficial and deep capillary networks of the telangiectatic vessels. There was also late intraretinal staining by fluorescein. The follow-up period was 19 months
4 for Case 1 and 11 months for Case 2.

The ocular examinations included measurements of the BCVA, ophthalmoscopy, fluorescein angiography (FA), and spectral domain optical coherence tomography (SD-OCT). Serial SD-OCT B-scan images were obtained with the Cirrus HD-OCT (Carl Zeiss Meditec, Dublin, CA, USA). The foveal thickness (FT) was measured as the distance between the internal limiting membrane and inner border of the retinal pigment epithelium at the foveal centre with the computer-based caliper built into the OCT system. The vertical and horizontal B-scan images across the fovea were used to
5 determine the foveal thickness.

3. Case Reports

3.1. Patient 1. A 79-year-old woman complained of blurred vision in her right eye and came to our clinic. Her BCVA was 20/100 OD and 20/25 OS. FA showed telangiectasia temporal to the fovea with pronounced fluorescein leakage in the late phase in the area of the telangiectasia. OCT showed cystoid macular edema (CME) in the area surrounding the leakage (Figure 1). The right eye was diagnosed with MacTel type 1 and received STTA, IVB twice, and focal PC through a slit lamp. These treatments failed to decrease the leakage on FA and resolve the CME. The BCVA was not improved.

After discussing the treatment options, the patient gave us an informed consent for PPV with a 25-gauge trocar system combined with the endolaser focal PC on the right eye. After core vitrectomy, a posterior vitreous detachment was created by suction through the vitreous cutter. The internal limiting membrane was made more visible with triamcinolone acetonide particle (Maqaid), and it was grasped and peeled with a microforceps. Then, focal PC was performed on the fluorescein leakage points with a 25-gauge endolaser probe and 100 to 120 mW power so that the focal retinal edema was treated.

After that, the CME decreased and the BCVA improved gradually to 20/25 in 3 months. The leakage of fluorescein was not present, the CME could not be detected in the

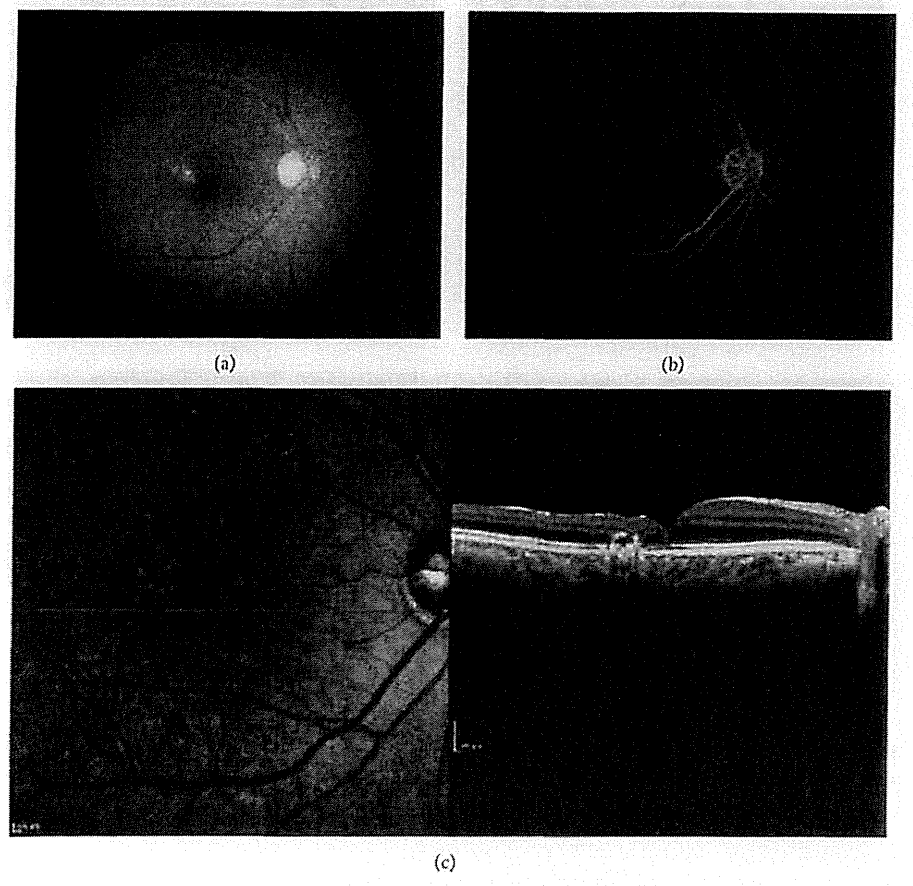

FIGURE 2: Findings of the right eye of Case 1 taken 3 months after surgery. The BCVA has improved to 20/25. (a) Fundus photograph showing localized area of scars from the laser photocoagulation temporal to the fovea. (b) Fluorescein angiogram showing the absence of fluorescein leakage in the late phase. (c) Optical coherence tomographic image showing an absence of cystoid macular edema and regained foveal pit.

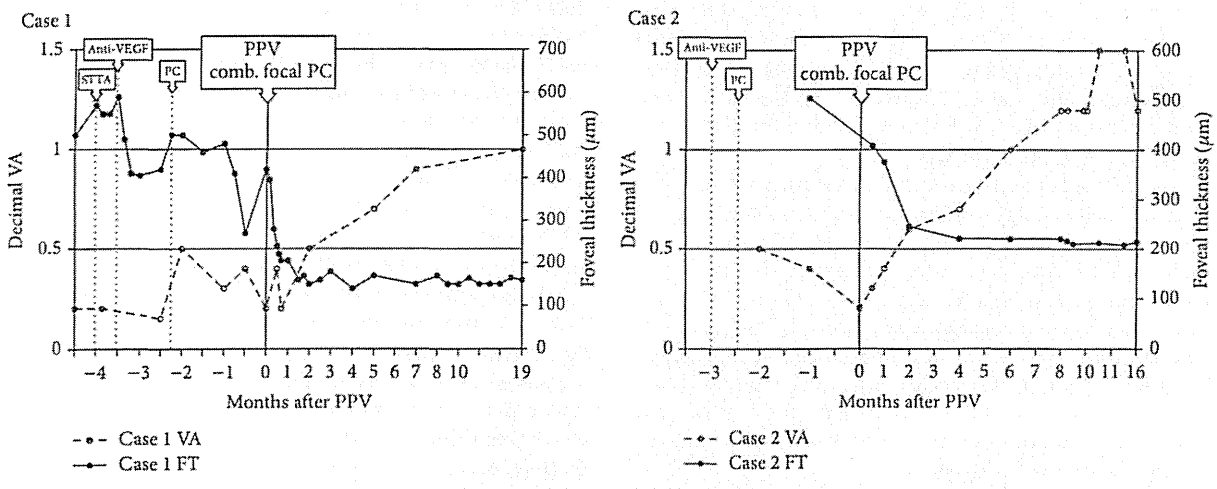

FIGURE 3: Clinical course of the affected eyes in two cases of MacTel type 1. In Case 1, the visual acuity improved to 20/20 and foveal thickness was reduced to 140 μm at 19 months after surgery. In Case 2, the visual acuity improved to 20/13 and foveal thickness to 208 um at 13 months after surgery.

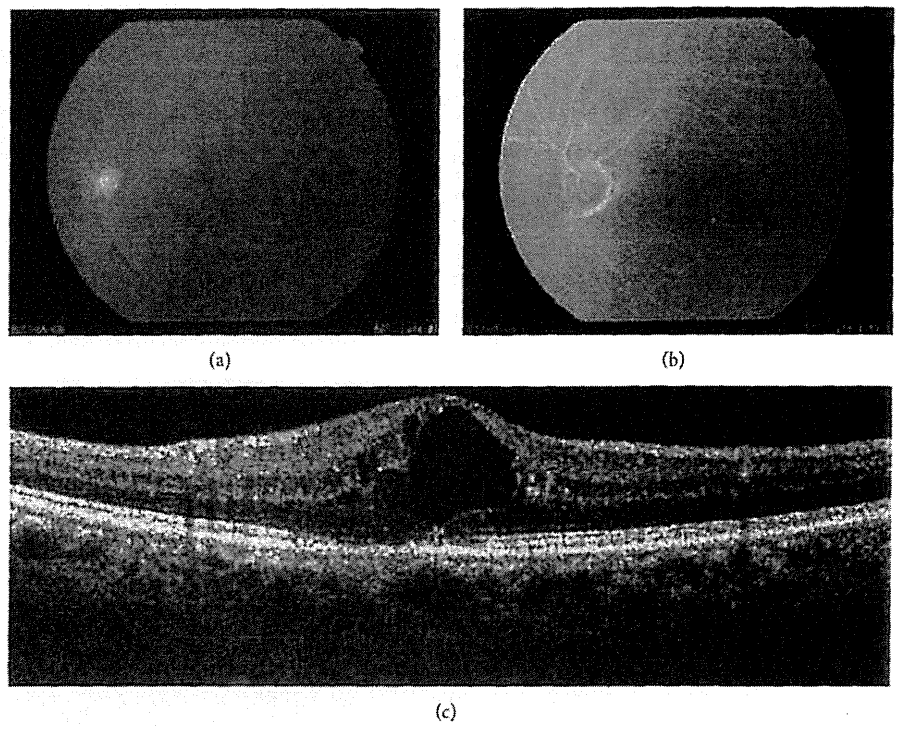

FIGURE 4: Findings of the left eye at the first visit of Case 2. The BCVA was 20/50. (a) Fundus photograph showed hard exudates associated with telangiectasia inferior temporal to the fovea. (b) Fluorescein angiogram showing fluorescein leakage in a circular pattern in the late phase. (c) Optical coherence tomographic image showed cystoid macular edema at the macula surrounded by circularly arranged fluorescein leakages.

OCT images, and the foveal thickness decreased from 420 to 140 μm (Figure 2). During the 19-month follow-up period, the BCVA and the CME progressively improved (Figure 3).

3.2. Patient 2. A 69-year-old woman with no relevant medical history presented with decreased vision in her left eye of 1-week duration. She had been diagnosed with macular oedema associated with MacTel type 1 and underwent IVB and focal PC in a private clinic. The treatments were not effective, and she was referred to us two months later.

Our examination showed that her BCVA was 20/20 OD and 20/50 OS. FA revealed ectatic capillaries temporal to the fovea with leakage in the late phase in both eyes but especially in the left eye. SD-OCT showed severe CME in the left eye (Figure 4). She was diagnosed with MacTel type 1 and underwent PPV with intraoperative endolaser focal PC as in Patient 1.

After that, the CME decreased and her BCVA improved gradually to 20/13 in 6 months. The leakage of fluorescein was not present, and the CME in the OCT images was not detected. The FT decreased from 512 μm to 200 μm (Figure 5). The clinical course of the left eye is showed in Figure 3. Nine months later, the right eye developed CME, but the BCVA remained at 20/20.

4. Discussion

Our results showed that PPV with endolaser focal PC can improve the BCVA and reduce the CME in patients with MacTel type 1. Our cases had not responded to focal PC through an integrated slit-lamp system, STTA, and/or antiangiogenic drugs, but after PPV with endolaser focal PC, the vision and CME improved. These findings strongly suggest a causal relationship between the treatment and the improvements.

Several treatments have been reported to be effective for MacTel, especially for type 2 [7, 8, 11], and there are few reports on the treatment of MacTel type 1 [4, 8–10]. IVTA or STTA has been reported to be effective in some cases [3–7] because steroids are anti-inflammatory and might maintain the blood-retina barrier. Recently, antiangiogenic drugs such as bevacizumab or ranibizumab have been reported to be effective in some cases of MacTel type 1 [8–10]. Antiangiogenic drugs are known to reduce neovascularization and oedema; however the follow-up times in those reports were relatively short and some cases had recurrences. Therefore, the efficacy of those therapies has still not been definitively determined.

At present, there is no consensus regarding the treatment of MacTel. Our two patients had no or only limited improvement clinically and angiographically after PC, STTA, and/or antiangiogenic therapy. Thus, we believed that intraoperative endolaser focal PC may be more effective because it allows

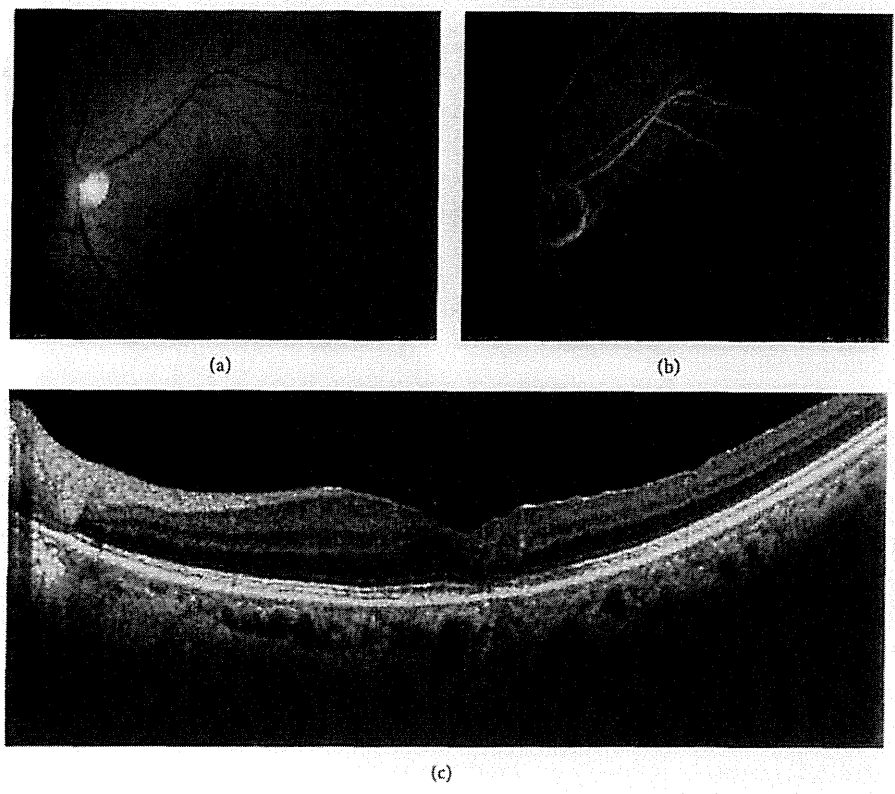

FIGURE 5: Fundus appearance of the left eye of Case 2 six months after surgery. Visual acuity has improved to 20/13. (a) Fundus photograph showed localized area of scarring by laser photocoagulation inferior-temporal to the fovea. (b) Fluorescein angiogram showing the disappearance of fluorescein leakage in the late phase. (c) Optical coherence tomographic image showing the absence of cystoid macular edema and restored foveal contour.

for better accuracy in treating the lesions than through an integrated slit-lamp delivery system. Focal PC through a slit lamp has several disadvantages. The site of the lesion can be easily affected by micromotions of the eye, the use of a joystick and manipulation of the contact lens require considerable technique and experience, reflected light from the contact lens can reduce the visibility of the macular region, and the endolaser beam can be delivered at different angles which can reduce the energy to the retinal pigment epithelium (RPE) over the fovea. The RPE is located in the outer layer and microaneurysm is in the inner layer, and the laser beam that is delivered obliquely from the inner and central side arrives relatively peripheral to the outer layer. This can prevent damage to the RPE. And finally, the endolaser procedure is not influenced by an opaque media, and the intravitreal laser probe can be brought very close to the retinal surface.

However, there are also drawbacks to the endolaser photocoagulation such as the difficulty for repeated treatments because of the risks associated with intraocular surgery.

There are several factors that may have played a role in improving the macular edema after PPV with endolaser focal PC. The removal of the vitreous and/or ILM may have reduced the level of pathological cytokines or chemical mediators adjacent to the telangiectasia. There are several reports showing that ILM peeling is effective treatment for macular edema secondary to diabetic retinopathy (DME) [12, 13] and retinal vein occlusion (RVO) [14]. Although the mechanism of the ILM peeling has not been fully understood, it might have contributed to the successful outcome. The intraoperative use of TA may have similar effect as STTA or IVTA although its use was only transient. The effectiveness of PPV alone can be assessed if intraoperative PC was not done. But the therapeutic protocol did not allow it. In addition, Sigler et al. reported that PPV was not effective against nonproliferative idiopathic MacTel type 2 [15]. MacTel type 1 is mainly exudative and nonfamilial, while type 2 is primarily nonexudative, obstructive, and occasionally familial. This may explain the differences of our results from the results of Sigler et al. In addition, some cases of MacTel type 1 respond well to antiangiogenic drugs but not type 2.

There are some limitations in our study. This was a retrospective study of only 2 patients. In addition, the follow-up period was short, and there were no controls. However, we believe that PPV with endolaser focal PC is effective and should be considered as an optional treatment for selected cases of MacTel type 1 especially in refractory cases. These treatment protocols should lead to an improvement in both the BCVA and macular edema.

In conclusion, we have experienced two patients with MacTel type 1 who were refractory to photocoagulation (PC),

STTA, and IVB but responded to pars plana vitrectomy (PPV) combined with intraoperative endolaser focal PC.

Although further investigations are needed to elucidate the rationale and to establish its indication, we think a stepwise approach to the management of the disease with the use of surgical management can be considered when conventional treatment fails.

Conflict of Interests

The authors declare that there is no conflict of interests regarding the publication of this paper.

Acknowledgments

No author has a financial or proprietary interest in any material or method mentioned. Support of this study was provided by Research Grants on Sensory and Communicative Disorders from the Ministry of Health, Labor, and Welfare, Japan.

References

[1] J. D. Gass and R. T. Oyakawa, "Idiopathic juxtafoveolar retinal telangiectasis," *Archives of Ophthalmology*, vol. 100, no. 5, pp. 769–780, 1982.

[2] J. D. M. Gass and B. A. Blodi, "Idiopathic juxtafoveolar retinal telangiectasis: update of classification and follow-up study," *Ophthalmology*, vol. 100, no. 10, pp. 1536–1546, 1993.

[3] L. A. Yannuzzi, A. M. C. Bardal, K. B. Freund, K.-J. Chen, C. M. Eandi, and B. Blodi, "Idiopathic macular telangiectasia," *Archives of Ophthalmology*, vol. 124, no. 4, pp. 450–460, 2006.

[4] A. Chopdar, "Retinal telangiectasis in adults: fluorescein angiographic findings and treatment by argon laser," *British Journal of Ophthalmology*, vol. 62, no. 4, pp. 243–250, 1978.

[5] Y. Hirano, T. Yasukawa, Y. Usui, M. Nozaki, and Y. Ogura, "Indocyanine green angiography-guided laser photocoagulation combined with sub-Tenon's capsule injection of triamcinolone acetonide for idiopathic macular telangiectasia," *British Journal of Ophthalmology*, vol. 94, no. 5, pp. 600–605, 2010.

[6] J. A. Martinez, "Intravitreal triamcinolone acetonide for bilateral acquired parafoveal telangiectasis," *Archives of Ophthalmology*, vol. 121, no. 11, pp. 1658–1659, 2003.

[7] K. K. W. Li, T. Y. H. Goh, H. Parsons, W. M. Chan, and D. S. C. Lam, "Use of intravitreal triamcinolone acetonide injection in unilateral idiopathic juxtafoveal telangiectasis," *Clinical and Experimental Ophthalmology*, vol. 33, no. 5, pp. 542–544, 2005.

[8] M.-A. Gamulescu, A. Walter, H. Sachs, and H. Helbig, "Bevacizumab in the treatment of idiopathic macular telangiectasia," *Graefe's Archive for Clinical and Experimental Ophthalmology*, vol. 246, no. 8, pp. 1189–1193, 2008.

[9] B. G. Moon, Y. J. Kim, Y. H. Yoon, and J. Y. Lee, "Use of intravitreal bevacizumab injections to treat type 1 idiopathic macular telangiectasia," *Graefe's Archive for Clinical and Experimental Ophthalmology*, vol. 250, pp. 1697–1699, 2012.

[10] A. Ciarnella, S. Verrilli, V. Fenicia et al., "Intravitreal ranibizumab and laser photocoagulation in the management of idiopathic juxtafoveolar retinal telangiectasia type 1: a case report," *Case Reports in Ophthalmology*, vol. 3, pp. 298–303, 2012.

[11] D. W. Park, H. Schatz, H. R. McDonald, and R. N. Johnson, "Grid laser photocoagulation for macular edema in bilateral juxtafoveal telangiectasis," *Ophthalmology*, vol. 104, no. 11, pp. 1838–1846, 1997.

[12] U. Mester and P. Dillinger, "Vitrectomy with arteriovenous decompression and internal limiting membrane dissection in branch retinal vein occlusion," *Retina*, vol. 22, no. 6, pp. 740–746, 2002.

[13] A. Gandorfer, E. M. Messmer, M. W. Ulbig, and A. Kampik, "Resolution of diabetic macular edema after surgical removal of the posterior hyaloid and the inner limiting membrane," *Retina*, vol. 20, no. 2, pp. 126–133, 2000.

[14] M. S. Mandelcorn and R. K. Nrusimhadevara, "Internal limiting membrane peeling for decompression of macular edema in retinal vein occlusion: a report of 14 cases," *Retina*, vol. 24, no. 3, pp. 348–355, 2004.

[15] E. J. Sigler, J. C. Randolph, J. I. Calzada, and S. Charles, "Comparison of observation, intravitreal bevacizumab, or pars plana vitrectomy for non-proliferative type 2 idiopathic macular telangiectasia," *Graefe's Archive for Clinical and Experimental Ophthalmology*, vol. 251, no. 4, pp. 1097–1101, 2013.

Composition Comments

1. Please check and confirm the author(s) first and last names and their order which exist in the last page.

2. Please check the correctness of the highlighted part.

3. Please provide valid postal codes to the addresses lacking ones.

4. We made the highlighted change for the sake of consistency. Please check similar cases throughout the paper.

5. We changed "Month after PPV" to "Months after PPV" in Figure 3 for the sake of clarity and consistency. Please check.

6. We reduced the font size of some labels in Figure 3. Please check.

7. We made the highlighted change for the sake of clarity and correctness. Please check.

Author(s) Name(s)

It is very important to confirm the author(s) last and first names in order to be displayed correctly on our website as well as in the indexing databases:

Author 1
Given Names: Gaku
Last Name: Terauchi

Author 2
Given Names: Celso Soiti
Last Name: Matsumoto

Author 3
Given Names: Kei
Last Name: Shinoda

Author 4
Given Names: Harue
Last Name: Matsumoto

Author 5
Given Names: Yutaka
Last Name: Imamura

Author 6
Given Names: Emiko
Last Name: Watanabe

Author 7
Given Names: Takaaki
Last Name: Kondo

Author 8
Given Names: Atsushi
Last Name: Mizota

It is also very important for each author to provide an ORCID (Open Researcher and Contributor ID). ORCID aims to solve the name ambiguity problem in scholarly communications by creating a registry of persistent unique identifiers for individual researchers.

To register an ORCID, please go to the Account Update page (http://mts.hindawi.com/update/) in our Manuscript Tracking System and after you have logged in click on the ORCID link at the top of the page. This link will take you to the ORCID website where you will be able to create an account for yourself. Once you have done so, your new ORCID will be saved in our Manuscript Tracking System automatically.

Hindawi Publishing Corporation
BioMed Research International
Volume 2014, Article ID 586060, 5 pages
http://dx.doi.org/10.1155/2014/586060

Hindawi

Research Article

Effect of Intraocular Lens Diameter Implanted in Enucleated Porcine Eye on Intraocular Pressure Induced by Scleral Depression

Gaku Terauchi,[1] Celso Soiti Matsumoto,[1,2] Kei Shinoda,[1] Harue Matsumoto,[2] and Atsushi Mizota[1]

[1] *Department of Ophthalmology, Teikyo University School of Medicine, 2-11-1 Kaga, Itabashi-ku, Tokyo 173-8605, Japan*
[2] *Matsumoto Eye Clinic, 50-2 Takagaki, Awa-cho, Awa-shi, Tokushima 771-1705, Japan*

Correspondence should be addressed to Kei Shinoda; shinodak@med.teikyo-u.ac.jp

Received 28 December 2013; Accepted 2 March 2014; Published 27 March 2014

Academic Editor: Toshihide Kurihara

The effect of the diameter of an intraocular lens (IOL) implanted in enucleated porcine eyes on the intraocular pressure induced by scleral depression was investigated. Two IOLs of 6 mm and 7 mm optic diameter were implanted. The intraocular pressure (IOP) was monitored during scleral depression by a transducer placed in the midvitreous through a sclerotomy at 6 o'clock. The area under the curve (AUC) of the IOP changes from the beginning of the indentation to the point when the peripheral retinal surface was observed through the IOL optics was measured. The AUC was significantly larger in eyes with a 6 mm IOL than in eyes with a 7 mm IOL ($p < 0.05$). The IOP elevation at the endpoint was higher in eyes with the 6 mm IOL than in eyes with the 7 mm IOL. We conclude that the AUC may represent the degree of stress induced by scleral depression. The higher AUC value with the X-60 may be because of the longer distance from the peripheral retina to the edge of the IOL optics.

1. Introduction

Small-incision cataract surgery and microincision transconjunctival vitrectomy have allowed combining pars plana vitrectomy with phacoemulsification and intraocular lens (IOL) implantation with less time and less invasion [1, 2]. In cases where the IOL is implanted first, the fundus visibility is improved by the clear IOL. However, the edge of the optics of the IOL can interfere with the observation of the equatorial and more peripheral areas of the retina. To overcome this limited view, scleral depression is used to observe the peripheral fundus [3, 4]. Scleral depression is a useful procedure; however, considerable pressure may be required to bring the peripheral retina and vitreous base into view. Scleral depression can be traumatic, because the eye is distorted and the intraocular pressure (IOP) is transiently elevated. However, the effect of scleral depression on the IOP has not been evaluated quantitatively.

Thus, the purpose of this study was to evaluate quantitatively the effects of the IOL diameter on the IOP induced by scleral depression to observe the peripheral fundus. To accomplish this, we implanted a pressure transducer in the vitreous and, also, implanted IOLs into enucleated porcine eyes. The IOP was then measured during scleral depression.

2. Materials and Methods

Combined pars plana vitrectomy, lens aspiration, and IOL implantation were performed on 4 enucleated porcine eyes (Figure 1). We implanted either the eternity X-60 or the eternity X-70 IOLs (Santen Pharmaceuticals, Osaka, Japan) into the porcine eyes. The diameter of the optics was 6.0 mm in the X-60 and 7.0 mm in the X-70 IOL. After the core vitreous was removed, a pressure transducer (Portable, 2-Channel, Serial Port I/O Module, Motorola Solutions Japan Ltd, Tokyo, Japan) was placed into the midvitreous through a sclerotomy at 6 o'clock. Scleral depression was performed at 10 mm posterior from corneal limbus at 3 or 9 o'clock. Constant pressure was delivered to the inner cylinder of a disposable 1cc syringe.

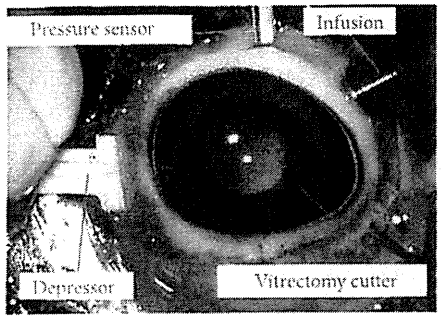

FIGURE 1: Photograph of enucleated porcine eye showing the experimental setup. After combined pars plana vitrectomy, lens aspiration, and IOL implantation, a pressure sensor was introduced into the vitreous cavity through a sclerotomy at 6 o'clock. Scleral depression was performed at 10 mm posterior from the corneal limbus at 3 or 9 o'clock.

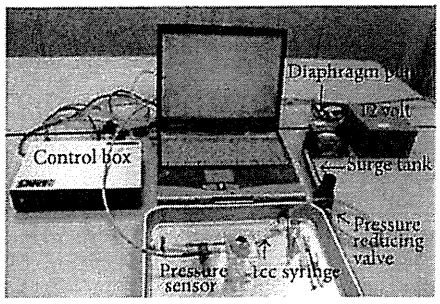

FIGURE 2: A custom made system to deliver constant pressure. Constant pressure (40 mm Hg) was delivered to the inner cylinder of a disposable 1cc syringe, which was used as a scleral depressor. And the external cylinder was held so that the tip of the inner cylinder was just touching the sclera 10 mm posterior from corneal limbus by surgeons.

And the external cylinder was held by surgeons (Figure 2). Physiological salt solution was used for the infusion solution, and the bottle height of the infusion was kept at 40 cm above the eye. To minimize the influence of the pupil diameter on the peripheral retinal observation through the optics, enucleated porcine eyes with similar pupil diameter was used. The apparent pupil diameter (mm) through cornea was 10.92 and 11.01 in eyes with X-60 and 10.96 and 10.98 in eyes with X-70.

The intraocular pressure (IOP) was monitored during scleral depression, in eyes with X-60, 9 times and, in eyes with X-70, 8 times. The IOP was measured from the beginning of the indentation to the endpoint when the peripheral retina was visible through the IOL optics. Then the IOP values were plotted as a function of time, and the area under the curve was determined.

2.1. Statistical Analyses. The AUC during scleral depression and the time from the beginning to the endpoint when the peripheral retina were visible through the IOL optics, and the IOP elevation at the endpoint was measured, unpaired t tests were used to determine the significance of the differences of these parameters between eyes with the eternity X-60 and the eternity X-70. A $p < 0.05$ was taken to be significant.

TABLE 1: Comparisons of the scleral depression parameters between eye with X-60 and X-70.

IOL size	AUC	Δt	ΔP
X-60	908.5 ± 244.1	9.8 ± 2.08	50.5 ± 4.51
X-70	303.5 ± 40.2	7.26 ± 1.11	37.0 ± 1.92
p	$p < 0.01$	$p = 0.29$	$p < 0.01$

Each value is shown as mean ± S.E.
IOL: intraocular lens, AUC: area under the curve.

3. Results

Representative graphs of the IOP change during sclera depression of the eye are shown in Figures 3 and 4. The mean ± standard error of the means (SEM) AUC was 908.5 ± 244.1 mm Hg sec in eyes with the eternity X-60 and 303.5 ± 40.2 mm Hg sec in eyes with the eternity X-70 ($p < 0.01$, Table 1). The time from the beginning to the endpoint when the peripheral retina was visible was 9.8 ± 2.1 sec in eyes with the X-60 and 7.3 ± 1.1 sec in eyes with the X-70 IOL ($p = 0.29$, Table 1) during the sclera depression when great care was taken to exert uniform pressure. The IOP elevation at the endpoint was 50.5 ± 4.5 mm Hg in eyes with the X-60 and 37.0 ± 1.9 mm Hg in eyes with the X-70 ($p < 0.01$, Table 1).

4. Discussion

Scleral depression is used to examine the peripheral retina and also during the shaving of the peripheral vitreous, endolaser photocoagulation of the peripheral retina, and dissection or removing of peripheral membranes. Although endoscopy can be used to avoid scleral indentation, it requires experience and skill. Another solution to the stress on the eye by scleral depression may be to perform the IOL implantation after the vitrectomy or selecting a large diameter IOL [5, 6]. Several authors have reported that an IOL with relative large diameter was advantageous, because the peripheral fundus was visible during the vitreous surgery [5, 6]. With smaller diameter IOLs, the fundus is viewed sometimes through the optics and other times around the optics. Thus, there is a need for continuous refocusing of the operating microscope.

The effect of the IOL diameter on the changes in the IOP induced by scleral depression had not been evaluated. Our results showed that the AUC was smaller and the time to reach the endpoint was shorter with the larger diameter IOL during scleral depression. This is probably because the distance between the peripheral retinal surface and the edge of the IOL optics is farther in eyes with the smaller diameter IOL, and, therefore, a deeper indentation is necessary to bring the peripheral retina into view through the IOL optics. Our results suggest that larger diameter IOL may be able to reduce the depth of scleral indentation, thereby, minimizing the stress on the eye during scleral depression.

Our findings suggest that the AUC may be used to determine the degree of stress on the eye during scleral depression.

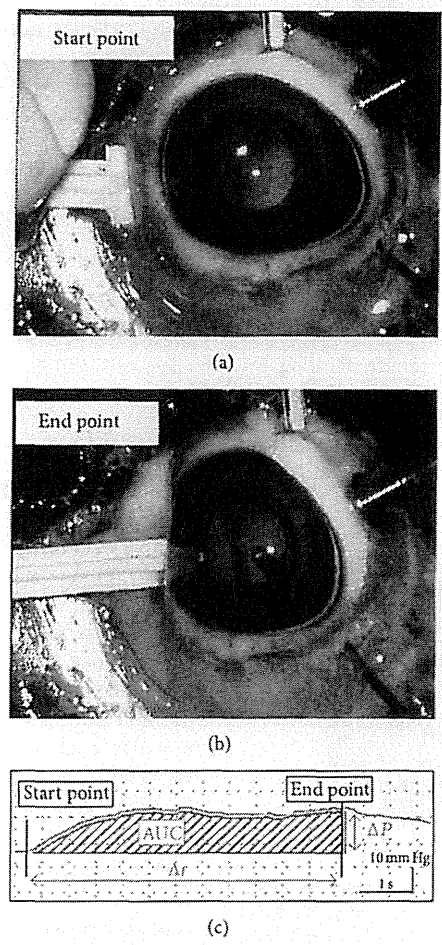

FIGURE 3: Representative graph showing IOP changes during scleral indentation in eye with X-60 implanted. (a) Scleral depression was performed at 10 mm posterior from the limbus at 3 or 9 o'clock. (b) Scleral depression was performed so that the peripheral retina can be seen through the optics of X-60 implanted in the anterior chamber. The markings of the graph show that the starting (arrowhead) and end (arrow) points of the scleral depression are shown in the lower figure. (c) Graph of the intraocular pressure (IOP) as a function of time during the scleral indentation. The area under the curve (AUC) of the IOP from the beginning of the indentation (start point) to the endpoint when the peripheral retinal surface was observed through the IOL was measured. Abscissa axis: time (0.5 seconds/scale), vertical axis: intraocular pressure (10 mm Hg/scale).

The system may also be used for surgeon's exercise for scleral depression.

There are some limitations in our study. Scleral depression was performed with great care to exert uniform pressure. But the speed and pressure depended on the surgeon's experience. The results showed that ΔP was significantly different between eyes with the X-60 and eyes with the X-70 IOL but Δt was not significantly different. This might suggest that the speed rather than the pressure was constant during depression. Constant pressure during scleral indentation by using a syringe pump like system would enable more precise comparison of the IOP change between each indentation. Due to the study design, the surgeon could not be masked to the type of IOL implanted. In addition, the IOP elevation during scleral indentation is influenced by several factors, such as the size of the eye, the rigidity of the eye wall, the position of the indentation, and the material filling the vitreous cavity. We believe that similar results can be observed in the clinical setting, because the size and rigidity of the eye of the porcine eye are not so different from the human eye. In our experiment, the scleral depression was done at 10 mm posterior from the limbus and the IOP change during indentation was measured after core vitrectomy. These procedures are similar to the clinical situation and care was taken to keep these factors constant. It would be interesting to measure the IOP change during scleral indentation when the vitreous cavity is filled with other materials such as air, silicone oil, and perfluorocarbon liquid or during fluid/air exchange.

Recently introduced vitrectomy system (Alcon Constellation Vision System) is equipped with a pressure control system and can maintain IOP at constant, independent of aspiration flow rates during vitrectomy. The IOP control system takes several seconds during the process of IOP detection and feedback [7]. Our system measures the IOP directly

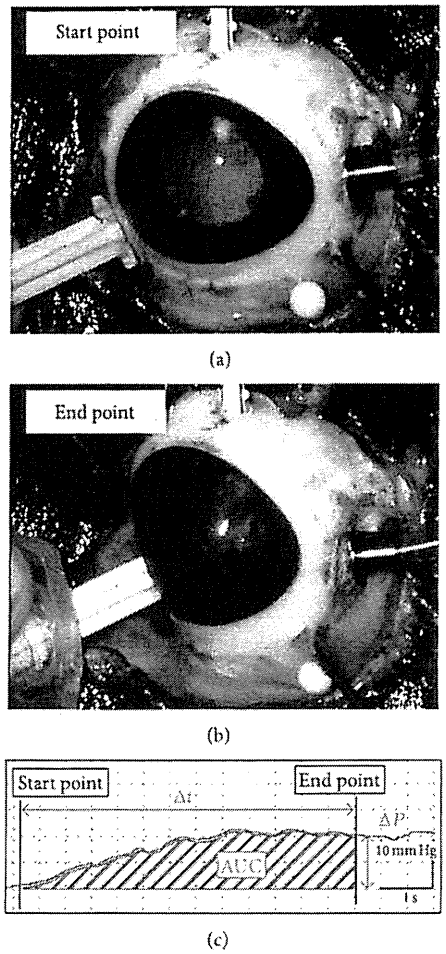

FIGURE 4: Representative plot of the IOP changes during scleral indentation in eye with X-70 IOL implanted. (a) Scleral depression was performed at 10 mm posterior from corneal limbus at 3 or 9 o'clock. (b) The scleral indentation was performed so that the peripheral retina can be seen through the optics of a X-70 IOL implanted in the anterior chamber. The markings of the plotting show that the starting (arrowhead) and end (arrow) points of the scleral indentation are shown in the lower figure. (c) Graph of the IOP as a function of time. The area under the curve (AUC) of the IOP from the beginning of the indentation to the endpoint when the peripheral retinal surface was observed through the IOL optics was measured. Abscissa axis: time (0.5 seconds/scale), vertical axis: intraocular pressure (10 mm Hg/scale).

and does not have such an inherent time lag. Sugiura et al. reported that IOP rapidly increased to 70–100 mm Hg and then slowly decreased to 30 mm Hg in 3.5–4.0 seconds during scleral depression without aspiration, with or without the IOP control system. If the IOP change against the time can be plotted, the AUC may be used as a parameter reflecting the degree of stress of the eye during vitrectomy maneuvers.

In conclusion, we were able to measure the IOP during scleral depression in enucleated porcine eyes implanted with different diameter IOLs. Analysis of the IOP changes clearly showed that an IOL with larger optics can minimize the effects of the scleral indentation.

Conflict of Interests

The authors declare that there is no conflict of interests regarding the publication of this paper.

Acknowledgments

No author has financial or proprietary interest in any materials or methods mentioned. Support of this study was provided by Research Grants on Sensory and Communicative Disorders from the Ministry of Health, Labor, and Welfare, Japan.

References

[1] V. Sood, R. Rahman, and A. K. Denniston, "Phacoemulsification and foldable intraocular lens implantation combined with 23-gauge transconjunctival sutureless vitrectomy," *Journal of Cataract and Refractive Surgery*, vol. 35, no. 8, pp. 1380–1384, 2009.

[2] H. Shinoda, K. Shinoda, S. Satofuka et al., "Visual recovery after vitrectomy for macular hole using 25-gauge instruments," *Acta Ophthalmologica*, vol. 86, no. 2, pp. 151–155, 2008.

[3] I. J. Constable and M. Nagpal, "Proliferative vitreoretinopathy," in *Retina*, S. Ryan, Ed., vol. 3, pp. 1807–1825, Elsevier, New York, NY, USA, 5th edition, 2008.

[4] T. G. Murray, H. C. Boldt, H. Lewis, G. W. Abrams, W. F. Mieler, and D. P. Han, "A technique for facilitated visualization and dissection of the vitreous base, pars plana, and pars plicata," *Archives of Ophthalmology*, vol. 109, no. 10, pp. 1458–1459, 1991.

[5] A. Watanabe, K. Okano, T. Shibata, H. Kato, and H. Tsuneoka, "Clinical efficacy of 7 mm intraocular lens for combined pars plana vitrectomy, phacoemulsifi cation and intraocular lens implantation," *J-Eye*, vol. 26, pp. 1413–1415, 2009 (Japanese).

[6] M. Wakabayashi, A. Imai, N. Kitazawa, D. Chiba, J. Arai, and T. Murata, "The Merits of 7.0 mm optics intraocular lens in phacovitrectomy," *Japanese Journal of Ophthalmology*, vol. 23, no. 1, pp. 121–124, 2010 (Japanese).

[7] Y. Sugiura, F. Okamoto, Y. Okamoto, T. Hiraoka, and T. Oshika, "Intraocular pressure fluctuation during microincision vitrectomy with constellation vision system," *American Journal of Ophthalmology*, vol. 156, no. 5, pp. 941–947, 2013.

Molecular Vision 2013; 19:1580-1590 <http://www.molvis.org/molvis/v19/1580>
Received 1 April 2013 | Accepted 15 July 2013 | Published 20 July 2013

Molecular characteristics of four Japanese cases with *KCNV2* retinopathy: Report of novel disease-causing variants

Kaoru Fujinami,[1,2] Kazushige Tsunoda,[1] Natsuko Nakamura,[1] Yu Kato,[1] Toru Noda,[1] Kei Shinoda,[3] Kaoru Tomita,[4] Tetsuhisa Hatase,[5] Tomoaki Usui,[6] Masakazu Akahori,[1] Takeshi Itabashi,[1] Takeshi Iwata,[1] Yoko Ozawa,[2] Kazuo Tsubota,[2] Yozo Miyake[1,7]

[1]National Institute of Sensory Organs, National Tokyo Medical Center, Tokyo, Japan; [2]Department of Ophthalmology, Keio University, School of Medicine, Tokyo, Japan; [3]School of Medicine, Teikyo University, Tokyo, Japan; [4]Heiwa Ganka Clinic, Tokyo, Japan; [5]Graduate School of Medical and Dental Sciences, Niigata University, Niigata, Japan; [6]Akiba Eye Clinic, Niigata, Japan; [7]Aichi Medical University, Aichi, Japan

Purpose: To describe the molecular characteristics of four Japanese patients with cone dystrophy with supernormal rod responses (CDSRR).

Methods: Four individuals with a clinical and electrophysiological diagnosis of CDSRR were ascertained. The pathognomonic findings of the full-field electroretinograms (ERGs) included a decrease in the rod responses, a square-shaped a-wave, an excessive increase in the b-wave in the bright flash responses, and decreased cone-derived responses. Mutational screening of the coding regions and flanking intronic sequences of the potassium channel, subfamily V, member 2 (*KCNV2*) gene was performed with bidirectional sequencing. The segregation of each allele was confirmed by screening other family members. Subsequent in silico analyses of the mutational consequences for protein function were performed.

Results: There were two siblings from one family and one case in each of the two families. One family had a consanguineous marriage. Mutational screening revealed compound heterozygosity for the two alleles, p.C177R and p.G461R, in three patients, and homozygosity for complex alleles, p.R27H and p.R206P, in one patient from the consanguineous family. There were three putative novel variants, p.R27H, p.C177R, and p.R206P. The four variants in the families with *KCNV2* were highly conserved in other species. In silico analyses predicted that all of the missense variants would alter protein function.

Conclusions: Biallelic disease-causing variants were identified in four Japanese patients with CDSRR suggesting that the pathognomonic electrophysiological features are helpful in making a molecular diagnosis of *KCNV2*. Three novel variants were identified, and we conclude that there may be a distinct spectrum of *KCNV2* alleles in the Japanese population.

Patients with cone dystrophy and supernormal rod electroretinograms (ERGs) were first reported in 1983, and the abnormality in the ERGs indicated a progressive degeneration of the cone photoreceptors associated with unique rod system abnormalities [1]. More detailed characteristics of this rare, autosomal recessive condition were reported in later studies, and the disease was named cone dystrophy with supernormal rod responses (CDSRR; MIM #610356) [2-8].

Most cases with CDSRR typically present in the first two decades of life with reduced visual acuity, abnormal color vision, and photophobia [8-11]. Night blindness is a later feature of the disorder [8]. The fundus appearance is variable, with some having a normal peripheral retina and a range of macular abnormalities [8-10]. The pattern of the autofluorescence (AF) images is also variable: Young cases have either a normal pattern or small parafoveal ring enhancements, while older cases have a narrow high-signal annulus that can encircle a central atrophic area of the retinal pigment epithelium (RPE) [6,12]. Recently, spectral domain optical coherence tomography (SD-OCT) and adaptive optics scanning laser ophthalmoscope (AOSLO) studies have described morphological changes of the fovea even at the early stages [10,13,14].

The electrophysiological findings are pathognomonic of CDSRR, and they assist in its early diagnosis [3,5,8-12,15-17]. The light-adapted ERGs are usually delayed and decreased in keeping with a generalized cone system dysfunction. There is also a unique rod system abnormality; the dark-adapted ERGs elicited by dim flashes are markedly decreased and delayed, and increasing the flash intensity results in an excessive increase in the b-wave amplitude accompanied by a shortening of the peak time of the b-wave [8,9,11]. A square-shaped a-wave trough of the dark-adapted bright flash ERGs is also a characteristic feature of this disorder [9,11].

Correspondence to: Kazushige Tsunoda, Laboratory of Visual Physiology, National Institute of Sensory Organs, 2-5-1 Higashigaoka, Meguro-ku, Tokyo 152-8902, Japan; Phone: +81334110111; FAX: +81334110185; email: tsunodakazushige@kankakuki.go.jp

CDSRR has been shown to be caused by mutations in the potassium channel, subfamily V, member 2 (*KCNV2*) gene (MIM# 607,604), which encodes a voltage-gated potassium channel subunit, Kv8.2 [18]. This silent subunit is expressed in rod and cone photoreceptors [18-20], and is thought to assemble with other K^+ channel subunits such as KCNB1, KCNC1, and KCNF1. These subunits form functional heteromeric channels with altered properties that have a narrowed membrane potential for activation and slow inactivation kinetics [19]. Eventually, these kinetic properties result in transient hyperpolarization overshoots on rapid changes in the inward currents [19]. A deficiency of Kv8.2 by a mutation in *KCNV2* may affect the characteristics of the I_{kx} as first described in amphibian photoreceptors [21]. This deficiency may influence the photoreceptor membrane potential. However, the underlying mechanisms that fully explain the clinical features of CDSRR are still not determined.

More than 50 different disease-causing variants in *KCNV2* have been reported: small insertion and deletion changes or large deletions that constitute a protein truncation and single nucleotide changes with amino acid substitutions [9,10,13,14,16,18,22,23]. Three small case series describe the clinical features of CDSRR in East Asians [3,5,15]; however, molecular genetic studies of these populations have not been published. Thus, the purpose of this study was to determine the molecular genetic characteristics from the clinical and electrophysiological findings of four Japanese patients who were diagnosed with CDSRR.

METHODS

Subjects: Four subjects who were diagnosed with CDSRR from the clinical and electrophysiological findings were ascertained at the National Institute of Sensory Organs, National Tokyo Medical Center, Tokyo, Japan and Niigata University, Niigata, Japan. The natural history of these four patients has been partially reported recently [24]. The procedures used were approved by the ethics committee of each institution, and all procedures were performed in accordance with the principles of the Declaration of Helsinki. Informed consent was obtained from all experimental subjects for all procedures.

Clinical assessment: A complete medical history was obtained, and a comprehensive ophthalmological examination was performed on all patients. The photophobia and night blindness episode was obtained on direct questioning. The clinical assessments included measurements of the best-corrected visual acuity (BCVA), dilated ophthalmoscopy, color fundus photography, AF imaging, OCT, and electrophysiological recordings. AF images were obtained with the HRA 2 confocal scanning laser ophthalmoscope (Heidelberg Engineering, Heidelberg, Germany; excitation light, 488 nm; barrier filter, 500 nm; field of view, 30×30°) [25]. The OCT images were obtained with SD-OCT (Cirrus HD-OCT, versions 4.5 and 5.1; Carl Zeiss Meditec, Dublin, CA) [26].

Electrophysiological assessments: Full-field ERGs were recorded from the four patients with the minimum standard protocol of the International Society for Clinical Electrophysiology of Vision (ISCEV) [27]. The ERG examination included the following: (i) dark adapted dim flash 0.01 $cd \cdot s \cdot m^{-2}$ (DA 0.01), (ii) dark adapted bright flash 30.0 $cd \cdot s \cdot m^{-2}$ (DA 30.0), (iii) light adapted 3.0 $cd \cdot s \cdot m^{-2}$ at 2 Hz (LA 3.0), and (iv) light adapted 3.0 $cd \cdot s \cdot m^{-2}$ 30 Hz flicker ERG (LA 3.0 30Hz). The extended protocol included the recording of the dark-adapted ERGs elicited by stimulus intensities of 0.001 $cd \cdot s \cdot m^{-2}$, 0.01 $cd \cdot s \cdot m^{-2}$, 0.3 $cd \cdot s \cdot m^{-2}$, 3.0 $cd \cdot s \cdot m^{-2}$, and 30.0 $cd \cdot s \cdot m^{-2}$. Two of the four patients were also recorded with the extended protocol. An excessive or disproportionate increase in the dark adapted b-wave with increasing flash intensity was assessed in these two patients, according to the previous report [9].

Mutational screening: After informed consent was obtained, blood samples were collected in EDTA tubes from each subject, and the DNA was extracted with a DNA extraction kit (QIAamp DNA Blood Maxi Kit; Qiagen, Venlo, the Netherlands). All exons and exon–intron boundaries were amplified with polymerase chain reaction (PCR), and the primer sequences used are shown in Table 1. PCR was performed with 20 µl volume containing 0.5 Unit Taq polymerase (PrimeStar GXL DNA polymerase, Takara, Tokyo, Japan). The sequence was determined based on the dideoxy terminator method using an ABI PRISM 3100×l Genetic Analyzer (Applied Biosystems, Foster City, CA) according to the manufacturer's protocol. The SeqScape Software version 2.5 (Applied Biosystems) was used to analyze the sequence alignment. Bidirectional Sanger sequencing was also performed in other family members of the proband, to confirm the segregation of the alleles.

Molecular genetic analyses: All of the missense variants identified were analyzed using two software prediction programs, Sorting Intolerant from Tolerance (SIFT) and PolyPhen2 [28,29]. The predicted effects on splicing of all missense variants were assessed with the Human Splicing finder program version 2.4.1. The allele frequency of each variant was estimated with the Exome Variant Server (NHLBI Exome Sequencing Project, Seattle, WA). A multiple sequence alignment program for DNA or proteins, the Clustal Omega, was applied to confirm an evolutionary conservation. Likely non-disease-causing variants (polymorphisms)

Table 1. Primer Sequences and Conditions for *KCNV2* Mutational Screening.

Primer	Sequence (5'–3')	Product size (bp)	PCR annealing (°C)
E1aF	AGGACCTGAGAAGGGGCAGCT	831	71
E1aR	TCCAGGAGGCGGAGGAACTCT		
E1bF	CCCTGCTGTCCACGCTGAATG	799	71
E1bR	CAGCGTGGGTAAGGTGGGTCA		
E1cF	AAGATCCAGCACGAGCTGCGC	841	65
E1cR	ATGGATGTCAAAAGTGGTGGA		
E2aF	AGCTTCTGTTCTTTTCATGAC	624	63
E2aR	GTCTCATAGTTGCTCTGTGTT		

bp = base pairs.

were also analyzed with the same protocol applied to likely disease-causing variants.

RESULTS

The demographic features of the four individuals from three families with CDSRR are summarized in Table 2. There were two siblings (patients 1 and 2) in one family and one case in each of the two families (patients 3 and 4). The pedigree of each family is shown in Figure 1, and a consanguineous marriage was present in family 3.

Clinical findings: The age of the patient at the time of the examination was 23, 17, 21, and 17 years with the age of disease onset at 9, 5, 3, and 2 years (Table 2). Three patients complained of photophobia (patients 1, 2, and 4), and all four patients had night blindness. Patient 4 had had mild nystagmus since age 2 years. The decimal BCVA of the four patients ranged from 0.08 to 0.8, and the BCVA of patients 1 and 2 was better than 0.7 in each eye.

The findings obtained from the color fundus photographs, AF images, and SD-OCT images are summarized in Figure 1 and Table 2. The fundus photographs showed mottling of the RPE at the macula in all four patients with subtle patchy granular flecks at the macula in patient 3. A ring enhancement of the AF signal was detected in the AF images of all four patients; three subjects had it centered on the fovea (patients 1, 2, and 3), and one had it at the parafovea (patient 4). In patient 3, the ring enhancement at the fovea was surrounded by patchy granular foci of the high AF signal at the macula.

SD-OCT demonstrated abnormalities in the outer retinal layers in all four patients. The cone outer segment tip line was absent in the macular area in all patients. The photoreceptor inner and outer segment junction line was discontinuous at the fovea in patients 3 and 4, and thinning of the outer retina was detected at the fovea in all four patients.

Electrophysiological assessments: The electrophysiological findings are summarized in Table 3, and the ERGs are shown in Figure 2. The full-field ERGs were recorded with the minimum ISCEV standard from patients 2 and 3, and extended protocol full-field ERGs including the dark-adapted ERGs elicited by an intensity series were obtained from patients 1 and 4.

The dark adapted b-wave amplitude elicited by a stimulus intensity 0.01 (DA0.01) was delayed and decreased in patients 3 and 4, but was normal but delayed in patient 1. The responses for DA0.01 were undetectable in patient 2. An excessive increase in the b-wave for the extended protocol was found in two patients, 1 and 4. In addition, the a-wave was square-shaped with a supernormal b-wave elicited by stimulus intensity 30.0 (DA 30.0) in all four patients. The photopic ERGs (LA 3.0 and LA 3.0 30Hz) were decreased in all four patients (Table 3 and Figure 2).

Molecular genetics: The molecular genetic findings are summarized in Table 2 and Appendix 1. Likely disease-causing variants in *KCNV2* were identified in all four patients. The four likely disease-causing variants were p.Arg27His, p.Cys177Arg, p.Arg206Pro, and p.Gly461Arg (Appendix 1), and two likely non-disease-causing variants (polymorphisms) were p.Gly61Gly and p.Ala265Ala (Appendix 2). The segregation of each allele was confirmed by screening of other family members for all these variants.

Detailed molecular results including in silico analysis to assist in predicting the pathogenicity of the four disease-causing variants identified are shown in Appendix 1. All of the four likely disease-causing variants were single nucleotide changes with one amino acid substitution (missense), i.e., p.Arg27His, p.Cys177Arg, p.Arg206Pro, and p.Gly461Arg. Compound heterozygosity for the two alleles, p.Cys177Arg and p.Gly461Arg, in patients 1, 2, and 3 and homozygosity for the complex alleles, p.Arg27His and p.Arg206Pro, in patient

Table 2. Summary of demographics, clinical findings and molecular status for four Japanese patients with *KCNV2*-retinopathy

Pt, FM, gender	Onset of disease, age at examination (years)	VA		Fundus		AF		OCT		Mutation status
		RE	LE	RPE mottling	Subtle patchy granular flecks	Ring enhancement	Patchy granular foci of high signal	Absence of COST	Deficit of IS/OS	
1, 1, F	9, 23	0.7	0.8	Macula	ND	Fovea	ND	Fovea	ND	Compund heterozygous [c.529 T>C, p.Cys177Arg]; [c.1381G>A, p.Gly461Arg]
2, 1, M	5,17	0.7	0.7	Macula	ND	Fovea	ND	Fovea	ND	Compund heterozygous [c.529 T>C, p.Cys177Arg]; [c.1381G>A, p.Gly461Arg]
3, 2, F	3,21	0.1	0.1	Macula	Macula	Fovea	Macuala	Macula	Fovea	Compund heterozygous [c.529 T>C, p.Cys177Arg]; [c.1381G>A, p.Gly461Arg]
4, 3, F	2, 17	0.1	0.08	Macula	ND	Para-fovea	ND	Macula	Fovea	Complex homozygous [c.80 G>A, p.Arg27His]; [c.617 G>C, p.Arg206Pro]

Pt = Patient; FM = family number; VA = logMAR visual acuity; RE = right eye; LE = left eye; RPE = retinal pigment epithelium; AF = autofluorescence; COST = cone outer segment tip line; IS/OS = photoreceptor inner and outer segment junction; ND = not detected. The affected area of each finding is based on the color fundus photographs, AF images, and the OCT images in each column.

Molecular Vision 2013; 19:1580-1590 <http://www.molvis.org/molvis/v19/1580>

Figure 1. Pedigree and retinal imaging of each patient with potassium channel, subfamily V, member 2 retinopathy. Pedigrees with molecular status of the three families with potassium channel, subfamily V, member 2 (*KCNV2*) retinopathy are shown on the left. Retinal images including color fundus photographs, autofluorescence images, and spectral domain optical coherence tomography are presented on the right. Images of patient 1 (top row), patient 2 (second row from top), patient 3 (third row from top), and patient 4 (bottom row) are shown.

4 were revealed by the segregation analyses. The p.Gly461Arg variant has been reported, and the p.Arg27His, p.Cys177Arg, and p.Arg206Pro variants are putative novel. In silico analysis revealed an "intolerant" protein function or a "probably or possibly damaged" protein but no effect on splicing in the three putative novel variants (SIFT, Poplyphen2, and Human Splicing finder; Appendix 1). The reported missense variant, p.Gly461Arg, with possibly affecting splicing was detected in six out of 13,006 individuals of the Exome Variant Server; the three novel variants, p.Arg27His, p.Cys177Arg, and